SIMULATION OF FUEL AND EMISSION BENEFIT ON A RANDOM SHIP VOYAGE BY POWERING THE AUXILIARY CONSUMERS WITH PEM FUEL CELL

Nikola Matulić, M.Eng.
University of Split, Faculty of Electrical Engineering, Mechanical Engineering and Naval Architecture, R. Boškovića 32, Split, Croatia, nimatuli@fesb.hr

Gojmir Radica, Ph.D. Professor
University of Split, Faculty of Electrical Engineering, Mechanical Engineering and Naval Architecture, R. Boškovića 32, Split, Croatia, goradica@fesb.hr

Nikola Račić, Ph.D. Associate Professor
University of Split, Faculty of Maritime Studies, R. Boškovića 37, Split, Croatia, nikola.racic@fesb.hr

ABSTRACT

The conventional marine propulsion systems are mainly equipped with diesel engines. The diesel engine does not only provide the thrust but also powers all other consumers on the ship. This results in high fuel consumption and pollutant production. Due to high fuel costs and stricter legislations, ship owners are forced to consider alternative, more efficient ways of powering their vessels. The technology that has a great potential in reducing the environmental impact of the transport sector is the hydrogen fueled polymer electrolyte membrane (PEM) fuel cell technology. The life cycle analysis of fuel cell propulsion systems as well as optimum integration strategy of the PEM fuel cell in hybrid systems is in the focus of today’s researchers. Numerous commercial propulsion systems are normally equipped with auxiliary power consumers that run on electricity. These auxiliaries usually have constant power demand which is delivered by the internal combustion engine, which results in increased diesel fuel consumption. In this research the commercial propulsion system powered by the diesel engine will be simulated on the random ship voyage, firstly with auxiliary loads powered by diesel engine and secondly with PEM fuel cell. The intention is to reduce cumulative fuel consumption and gaseous emissions by shifting the power production for auxiliary loads from the internal combustion engine to PEM fuel cell unit.

Keywords:
marine propulsion simulation, marine engine model, system simulation, PEMFC, auxiliary load

1 INTRODUCTION

Efficient zero emission ships are important for the future sustainable development. Fuel cell systems are considered for powering future ships in an efficient and low emitting manner, as they are environmentally friendly source of energy due to their superefficient use of fuel for electricity and heat. Fuel cell devices, particularly Proton Exchange Membrane (PEM) type, are strong candidates for replacing internal combustion engines in the transport industry (Alaswad, 2016). The electrical energy conversion efficiency of most fuel cells ranges between 40% and 60% based on the lower heating value (LHV) of the fuel (El-Gohary, 2007, 2008; Hordeski, 2008). Fuel cell emission levels will be accepted by the required international marine regulations addressed by the International Maritime Organization (IMO) and the International Convention for the Prevention of Pollution from Ships (MARPOL). The parameters, which affect fuel cell performance, include the number of cells, cell voltage, open cell voltage, fuel cell efficiency, and fuel utilization coefficient. The actual polymer electrolyte membrane (PEM) cell voltage is 0.868 volt and the open cell voltage is 1.031 volt. These two values affect the efficiency and performance of the fuel cell. Also, fuel utilization coefficient determines the amount of hydrogen consumption in the fuel cell and also affects the cell’s efficiency. The percentage of the power lost in heating for a fuel cell power plant is much less than that of the diesel generator and micro gas turbine. The use of a diesel generator or micro gas turbine will increase the fuel energy consumption rate by 23.59%, i.e. 43.95% more than that of the fuel cell fuel energy consumption at full load for the same output power (Yousri M. A., 2013). There are various possible marine applications. Standard distributed electricity or emergency electrical requirements can be generated by fuel cells systems (Jose J., 2016). While fuel cell use in the civilian and military surface ships is still at the investigation and demonstration stages, PEM fuel cells using hydrogen and oxygen have achieved serious maturity in submarines (Sattler et al., 2000). The results of the comparison of a high-speed hydrogen PEM fuel cell ferry and a ferry powered by the traditional diesel engine Tier 4 compline technology, show that operating a hydrogen fuel cell ferry on nearly 100% renewable hydrogen provides the reduction in GHG and pollutant emissions (Klebanoff L. E., 2017). The problems of global climate change and marine air pollution worldwide can be reduced with the help of this technology. The development and demonstration of a PEM fuel-cell-battery hybrid system for the propulsion of a 20-m-long tourist boat revealed a reliable operation of the fuel-cell battery hybrid system and boat speeds of 6.6-7.8 knots at a power output of ~85 kW (Choeng, 2016.). On sailing yachts, the consumption of electrical power is very restricted during long cruises because of low battery capacities. In this case, an additional power supply based on the noiseless fuel cell technology promises an essential comfort increase without disturbing emissions (Beckhaus, 2005). The so-called auxiliary power units (APU), suitable for a large scale of applications, ranging from power-driven automobiles and leisure applications to stationary uninterruptible power supply devices (UPS), are in the focus of fuel cell engineering. Auxiliary power units (APUs), i.e. devices designed to provide additional power in vehicles, are believed to be an important entry point for fuel cell (FC) technology into commercial markets. Three technologies are under consideration for this market: solid oxide fuel cells (SOFCs), proton exchange membrane fuel cells (PEMFCs) and direct methanol fuel cells (DMFCs). (Agnolucci, 2007). A data-validated power-efficiency model of a diesel-powered fuel-cell-based auxiliary power unit (APU) system has been investigated for the various sizes of the power unit and evaluated for the optimal choices for specified load profiles (Pregelj 2016). The challenge came from the FCGEN (Fuel Cell-based power GENeration) EU FP7 project, where such an APU was developed. The relation for optimal combinations, in terms of efficiency and degradation, is proposed and the confronted tradeoffs are discussed.

This paper aims at introducing a good solution for replacing the conventional marine power plants or for co-working with them. This implies the use of a fuel cell power plant operated on hydrogen produced through water electrolysis. This research provides a simulation of a commercial vessel fitted with a diesel engine operating under realistic conditions of a realistic voyage, with and without the auxiliary loads necessary for the analysis of fuel consumption increase. The increase in the fuel consumption and emissions will be reduced by shifting the power production for auxiliary loads from internal combustion engine to PEM fuel cell unit.

2 MARINE DIESEL ENGINE LOCAL FERRY RUN SIMULATION

A simulation model was built for demonstrating the benefit of using PEM fuel cell over the consumed fuel of the internal combustion engine. The simulation model was built using Cruise m simulation tool. For this purpose, Caterpillar C32 engine was chosen for the analysis. The engine is V12, 32.1 liter 500kW at 1800 rpm, with the bank separate turbocharging (2 turbochargers), electronically controlled injection. For this application, the load is following the propeller curve as shown in Figure 1.

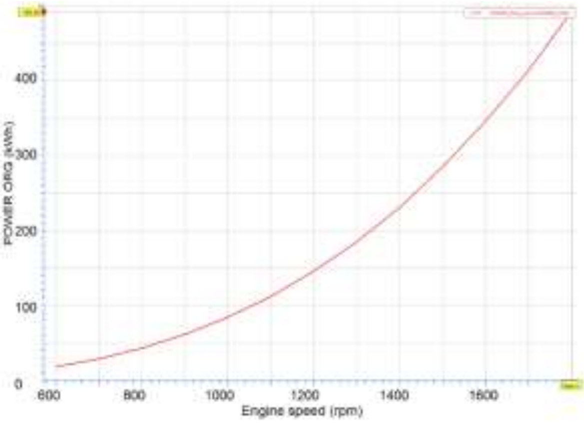

Figure 1: Propeller curve

The simulation model was built using main geometrical data such as the bore of 145 mm, stroke of 162 mm and compression ratio of 15. The rest of the geometrical data such as port dimensions, intake, exhaust, charge air cooler and air filter dimensions were assumed based on experience. The model was calibrated with experimental data obtained from the testbed: measurements of pressures and temperatures measured in intake and exhaust ports, fresh air mass flow, fuel flow, torque and emissions over the engine load range from 3% to 100%. For modelling the working fluid, the quasi-zero-dimensional model of components is used. Static parameters are determined using filling and emptying method coupled with the energy balance. Dynamic parameters are determined by flow equations that need to be followed with an adequate flow coefficient representing the pressure drop over the specific component. The turbocharger model is defined by the compressor and turbine mass flow and efficiency maps measured on the turbocharger hot-bench. The cylinder model consists of the intake and exhaust port model, injector model, heat transfer model that includes the piston, cylinder head and liner, and combustion chamber model (Figure 2).

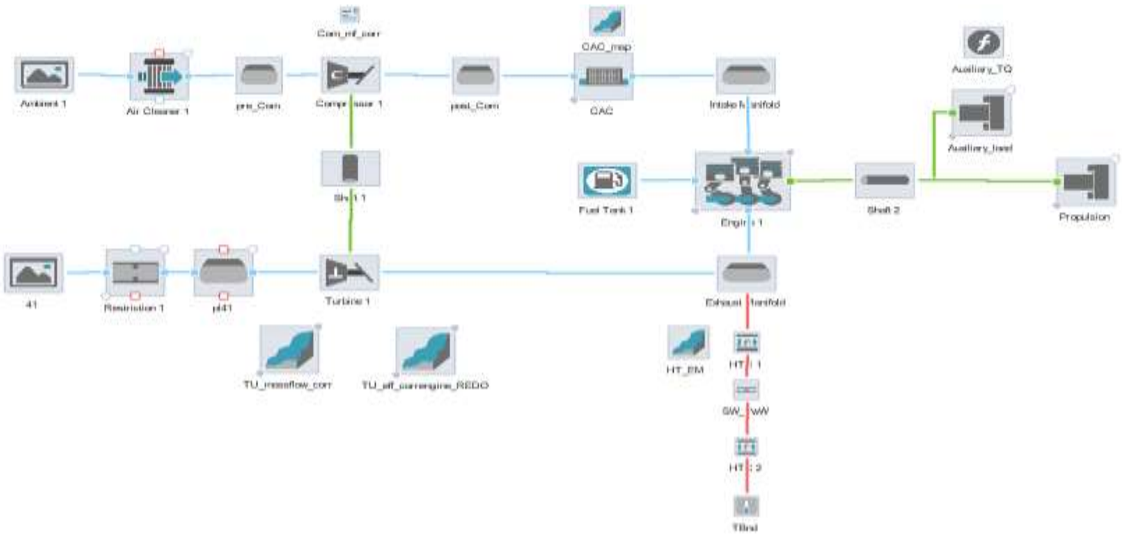

Figure 2: Cylinder model component overview

Part models are dynamic parameters determined by the valve lift profiles and timings as well as the flow coefficients. The injection model is made of rail and injector models. They are defined by geometry, injection signals and profiles. The injection process is defined with reference to the crank angle. The rail model is a 0D volume based model that considers the compressibility of the fluid. The approach used for injector rate determination is based on the injection velocity and nozzle area. The flow coefficients include the friction and are introduced into the model over the hole and needle seat area.

The combustion chamber model is in the function of the crank angle and consists of combustion and emission models. The combustion model used for this application was AVL Mixture-Controlled 2014 divided into the sub-models including the ignition delay, premixed combustion, diffusion combustion and wall impingement. It is a two zone combustion model. There are 3 pollutant formation models available, NOx, CO and Soot production models.

2.1 MODEL CALIBRATION

For the calibration purposes, the model was divided into two standalone models. This approach achieves the better results correspondence to the measurement of each component individually, without affecting the deviations caused by neighboring components in the system simulation. The first standalone model is the cylinder model where the states around the cylinder such as pressures, temperatures and mudflows, are stimulated from the measurements. The cylinder standalone calibration was divided into the three groups. The first group is the motoring phase where the fresh air mass flow is stimulated and the intake flow port parametrization is performed to match the intake manifold pressure to the measured one. After matching the port size, the friction mean effective pressure multiplier is also adjusted to achieve the desired engine model friction. In the second phase or group, the amount of the injected fuel needs to be matched to the testbed measurements by adjusting the fuel multiplier in the injector element model. When the air and fuel massed are matched, the next step involves the combustion parameters adjustment, for reaching the torque measured on the engine test bed. The adjusted parameters for the ignition delay model are of Arrhenius and Magnussen multiplier type. Higher values lead to reduction in the ignition delay. For premixed combustion, two parameters are available: the premixed fuel fraction that defines burned fuel fraction during ignition delay, and the combustion parameter that is a multiplier on the heat release rate in the premixed phase. For the diffusion combustion phase, three parameters are available. The combustion parameter is a multiplier on a heat release rate in the diffusion combustion phase, the spray lambda limit defines fuel fraction in the lambda distribution in spray model that is available for the combustion, and the turbulence parameter is the scaling factor for the kinetic energy in the spray. Finally, the wall impingement has two adjustments. The penetration length defines the free spray length into the combustion chamber and the reduction multiplier is the scaling factor of the wall impingement on the combustion rate.

After adjusting the combustion to fit the measured engine torque, the exhaust temperature at the exhaust port and in the exhaust manifold will be higher than the one on the testbed because of the influence of the heat transfer from the heat rejected between exhaust port and temperature sensor location. This effect was also modeled to fit the exhaust manifold temperature to the measured one.

For the turbocharger standalone model the goal is to achieve the desired boost pressure and temperature as well as the realistic backpressure, under test conditions stimulated from the measurements.

In the following figures, the simulation results are shown in blue color and measurements from the engine testbed in red color.

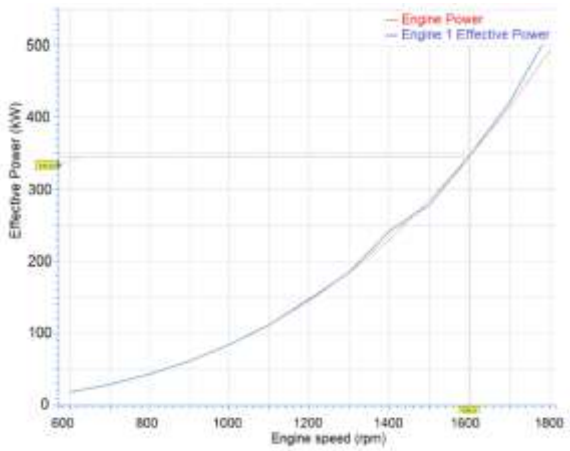

Figure 3: Power simulation result quality

Figure 3 shows the simulation results of the power output of the engine model compared to measurements results. Maximum deviation in the simulated power output is 5.5 % at full load point.

Maximum deviation in simulated intake manifold pressure output is 2 kPa at low load.

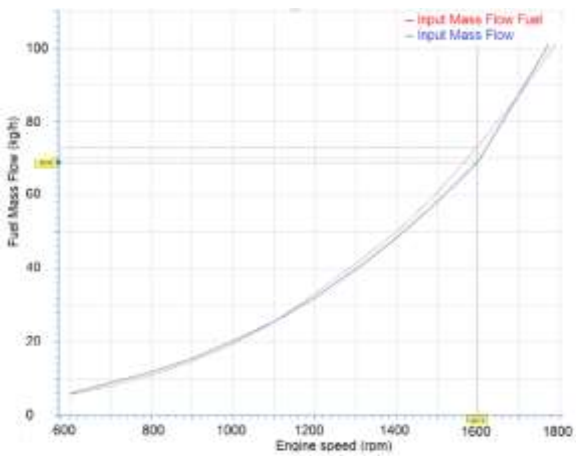

Figure 4: Fuel consumption simulation result quality

Figure 4 shows the simulation results of the fuel mass flow from the injection model, compared to measurement results. Maximum deviation in the simulated fuel flow output is 5.5 %. The fuel amount deviation is also causing deviation in the power output and in exhaust temperature. It can be further improved but here it represents a high model quality.

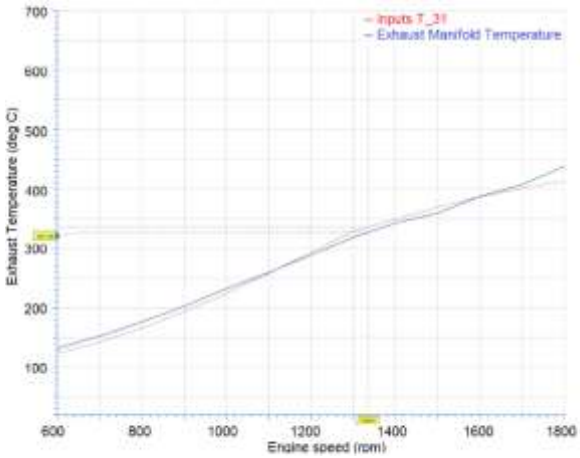

Figure 5: Exhaust temperature simulation result quality

Figure 5 shows the simulation results of the exhaust temperature compared to measurement results. Maximum deviation in simulated exhaust temperature is 10°C or 3.1%.

The simulation results have showed a high model quality and good model interpolation capability that also points to a robust model calibration parameters.

2.2 FUEL AND EMISSION BENEFIT SIMULATION

After calibration of the engine model according to the testbed data, the realistic voyage profile was simulated to estimate the amount of consumed fuel and CO_2 emissions during the local ferry one-hour run. It is assumed that the sea is calm. The engine load profile is: 5% load for 5 minutes during maneuvering in the port, raising the load from 5% to 80% in 2.5 minutes, sailing under 80% of load for 45 minutes and then derating to 5% for entering the next port of call in 2.5 minures and at 5% load for port maneuvering during 5 minutes (Figure 6.).

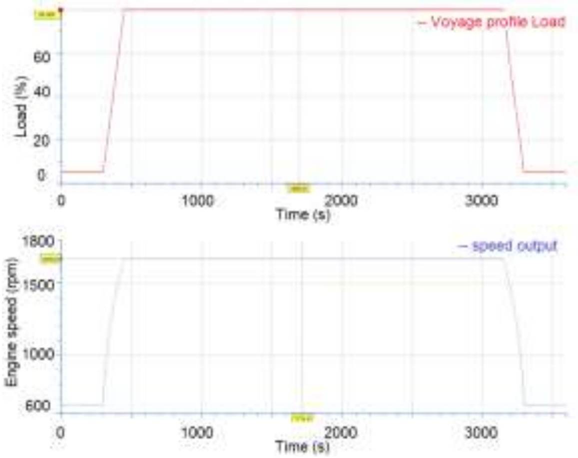

Figure 6: Engine speed and load profile during 1 hour voyage

During the 1-hour voyage, the generator on the shaft was mounted for supplying power to the auxiliary consumers on the ship. The power demand on the generator for auxiliary consumers power supply is based on using the fraction of engine produced power and it is showed in Figure 7.

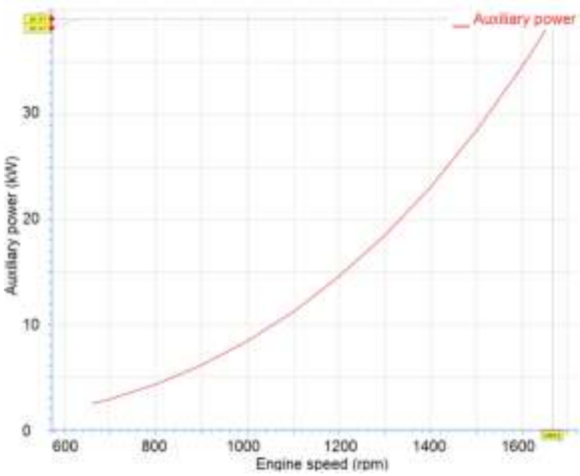

Figure 7: Auxiliary power demand for external consumers on the ship during the defined voyage

Figure 7 indicates that at 80% of the engine load the power demand for auxiliary consumers reaches 40 kW and at 100% load the auxiliary power demand rises up to 50 kW.

The voyage simulation was performed two times. Once simulation setup included the shaft generator at the engine front, for supplying auxiliary power demand to additional consumers on the ship, and the second simulation was performed under assumption that auxiliary power demand is supplied by an external power source such as fuel cell. By removing auxiliary power demand from the internal combustion engine, the load is decreased and fuel consumption and emissions are reduced.

In the following figures the blue color represents the voyage simulation with auxiliary power demand supplied by the internal combustion engine, while the red color represents the voyage simulation with auxiliary power demand supplied by an external power source such as fuel cell.

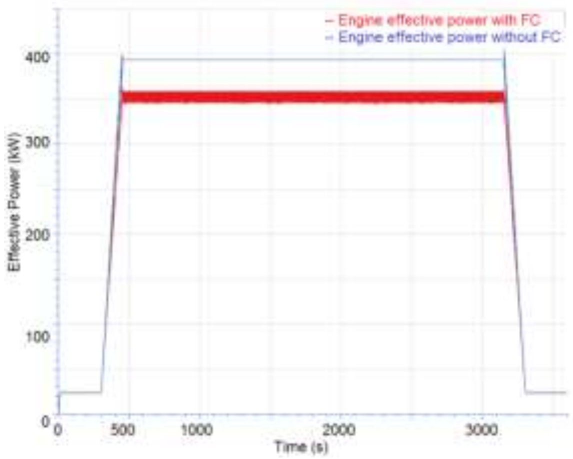

Figure 8: Engine power reduction due to the external power supply for auxiliary demand during the voyage

Figure 8 shows that during the voyage when power for auxiliary consumers is supplied from fuel cell, the decrease in internal combustion load is about 10%. This leads to reduction in fuel consumption and has a significant impact on emissions reduction, without influencing the voyage duration. Additionally, the intake manifold pressure was reduced by 20 kPa and the exhaust manifold temperature by 25°C, which implies a positive reduction in thermal load.

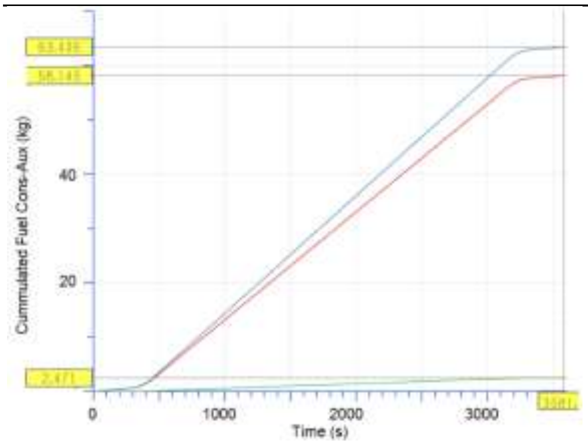

Figure 9: Cumulated fuel reduction due to the external power supply for auxiliary demand during the voyage

By excluding the load for powering auxiliary consumers from the internal combustion engine, at the end of 1 hour voyage, a fuel consumption decrease of almost 5.26 kg, or nearly 9% less diesel fuel consumption, is achieved by using 2.47 kg of hydrogen (Figure 9.). Since the ferry uses 4 identical main engines and sails 16 hours per day, this results in a fuel saving up to 336 kg of diesel fuel per day.

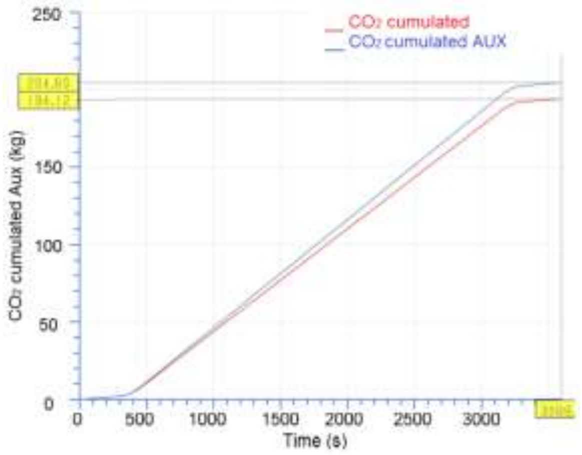

Figure 10: Cumulated CO_2 reduction due to external power supply for auxiliary demand during the voyage

Figure 10 shows the reduction in cumulated CO_2 emissions by 5.5%. Per 4 engines and 16 hours of sail per day, the reduction of CO_2 amounts to 670 kg per day.

3 FUEL CELL CALCULATION FOR POWERING AUXILIARY LOADS

Polymer electrolyte membrane (PEM) fuel cells are chosen as optimal solution for this application due to delivery of high power density with low weight compared to other fuel cell technologies.

PEM fuel cells are mostly used in transportation due to fast readiness for operation and low weight compared to other fuel cell technologies. The PEM fuel cell system calculation was performed and the stack was defined for this case with the maximum power supply of 50 kW.

The power of the fuel cell is calculated by:

$$P = I \cdot V_{stack} \qquad (1)$$

Where P is the power, I is the current and V_{stack} is the voltage of the fuel cell stack. Current is given by:

$$I = iA \qquad (2)$$

Where i is current density and A is the stack surface. The voltage of the stack is defined by:

$$V_{stack} = NV_{cell} \qquad (3)$$

Where N is number of cells in the stack and V_{cell} is the voltage of the cell. The voltage of the cell can be described as:

$$V_{cell} = V_{th} - \frac{RT}{\alpha F}\left(\frac{i}{i_0}\right) - iR_i \qquad (4)$$

Where V_{th} is the theoretical cell voltage, R is gas constant, T is the operating temperature, α is charge transfer coefficient, F is Faraday´s constant, i_0 is the exchange current density and R_i is the resistance. Theoretical voltage can be expressed as:

$$V_{th} = -\left(\frac{\Delta H}{nF} - \frac{T\Delta S}{nF}\right) + \frac{RT}{nF}\ln\left(\frac{P_{H_2}P_{O_2}^{0,5}}{P_{H_2O}}\right) \qquad (5)$$

Where ΔH is the heat of formation, ΔS is entropy, n is number of electrons per molecule and P_x are partial pressures.

The cell characteristic is defined by the cell polarization curve. The standard polarization curve available from manufacturer was chosen (Figure 11) and the number of cells was adjusted to fit the needs of the power for auxiliary consumers on the ship (Figure 12).

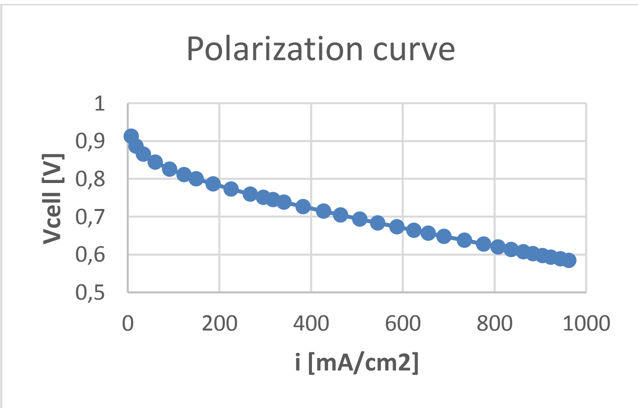

Figure 11: PEM fuel cell polarization curve

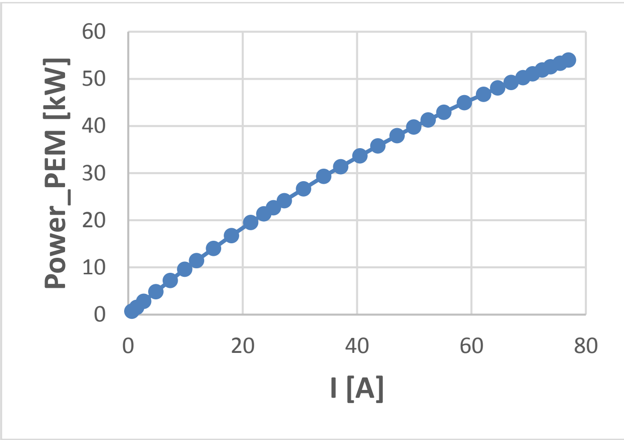

Figure 12: PEM fuel cell power curve

4 CONCLUSION

Since the auxiliary onboard loads such as cooling systems, ventilation, hydraulic pumps and others are powered by diesel-generator sets and sometimes by using the shaft generator attached to the propulsion engine, they consume fuel and produce pollutants. In this paper, the propulsion engine fitted with the shaft generator was analyzed. The auxiliary power demand implies extra load on the propulsion engine and increases fuel consumption, especially in port where the propulsion engine runs at low loads, which is the most inefficient mode of diesel engine operation. The fuel cell stack was designed to meet maximum 50 kW of the auxiliary power demand. When the auxiliary power demand for the ship consumers was taken off the internal combustion engine, the simulation showed benefits in fuel consumption and pollutant production on a realistic voyage. During the 16 hours of the simulated ferry's sailing in calm sea condition, the fuel saving was up to 336 kg which resulted in the reduction of 670 kg CO_2 per day. The diesel fuel consumption was decreased by 9% and CO_2 emissions reduced by 5.5 %.

Further steps would be to calculate the hydrogen tank capacity for certain voyage or to do the economic analysis of the electrolyzer installation, and to perform a feasibility study of the whole system.

REFERENCES

[1] A. Alaswad, A. Baroutaji, H. Achour, J. Carton Ahmed Al Makky, A. G. Olabi, Developments in fuel cell technologies in the transport sector, International journal of hydrogen energy 41 (2016) 1649-16508

[2] El-Gohary, M. M., 2007. Design of Hydrogen Marine Gas Turbine. *Alexandria Engineering Journal*, 45, pp. 42-53.

[3] El-Gohary, M. M., 2008 Design of Marine Hydrogen Internal Combustion Engine. *Alexandria Engineering Journal*, 47(1), pp. 57-65.

[4] Hoogers, G. (ed.), 2003. *Fuel Cell Technology Hand Book*. London New York Washington: CRC Press. 0-8493-0877-1, pp. 8-30.

[5] Yousri M., A. Welaya, M. Morsy El Gohary and Nader R. Ammar, A comparison between fuel cells and other alternatives for marine electric, Inter J Nav Archit Oc Engng (2011) 3:141-149

[6] Jose J. de-Troya, Carlos Alvarez, Carlos Fernandez-Garrido, Luis Carral, Analysing the possibilities of using fuel cells in ships, International journal of hydrogen energy 41 (2016) 2853-2866

[7] Sattler G. Fuel cells going on-board. J Power Sour 2000;86:61e7. http://dx.doi.org/10.1016/S0378-7753(99)

[8] L. E. Klebanoff, J. W. Pratt, C. M. Leffers, K. T. Sonerholm, T. Escher, J. Burgard, S. Ghosh, Comparison of the greenhouse gas and criteria pollutant emissions from the SF-BREEZE high-speed fuel-cell ferry with a diesel ferry power generation, Transportation Research Part D 54 (2017) pp. 250–268

[9] Choeng Hoon Choi, Sungju Yu, In-Su Han, et al., Development and demonstration of PEM fuel-cell-battery hybrid system for propulsion of tourist boat, International journal of hydrogen energy 41 (2016) 3591-3599

[10] P. Beckhaus, M. Dokupil, A. Heinzel, S. Souzani, C. Spitta, On-board fuel cell power supply for sailing yachts, Journal of Power Sources 145 (2005) pp. 639–643

[11] P. Agnolucci, Prospects of fuel cell auxiliary power units in the civil markets, International Journal of Hydrogen Energy 32 (2007) 4306 – 4318

[12] B. Pregelj, M. Micor, G. Dolanc, J. Petrovcic, V. Jovan, Impact of fuel cell and battery size to overall system performance – A diesel fuel-cell APU case study, Applied Energy 182 (2016) pp. 365–375.